

High-current long-duration uniform electron beam generation in a diode with multicapillary carbon-epoxy cathode

T. Queller, J. Z. Gleizer, and Ya. E. Krasik
Physics Department, Technion, Haifa 32000, Israel

(Received 6 April 2013; accepted 9 September 2013; published online 30 September 2013)

The results of reproducibly generating an electron beam with a current density of up to 5 kA/cm^2 , without the cathode-anode gap being shorted by the plasma formed inside the cathode carbon-epoxy capillaries, in a $\sim 350 \text{ kV}$, $\sim 600 \text{ ns}$ diode, with and without an external guiding magnetic field, are presented. The cathode sustained hundreds of pulses without degradation of its emission properties. Time- and space-resolved emissions of the plasma and spectroscopy analyses were used to determine the cathode plasma's density, temperature, and expansion velocity. © 2013 AIP Publishing LLC. [<http://dx.doi.org/10.1063/1.4822019>]

I. INTRODUCTION

There is continuous interest in cathodes that can be used for the generation of pulsed electron beams that have an electron energy above 100 keV , are uniform in the cross-sectional area at a current density exceeding 100 A/cm^2 , and whose duration is longer than 10^{-7} s . These electron beams can be used to generate intense x-ray fluxes, pump high-pressure gaseous lasers, and generate powerful microwaves. The source of electrons for such high-current electron beams is either explosive emission plasma,¹ flashover plasma, or plasma formed prior to the application of the accelerating pulse by gas ionization inside the cathode. The present status and a review of the different cathodes and their emission mechanisms, along with their relative advantages and disadvantages for generating intense electron beams, can be found in Refs. 2 and 3. However, plasma cathodes that show good emission parameters (reliability, reproducibility, and long lifetime) for the generation of electron beams with a current density $\leq 100 \text{ A/cm}^2$ have not been used to generate electron beams with a larger current density, because of either insufficient plasma density or their short lifetime. Thus, only explosive emission plasma cathodes are considered for generating electron beams with current densities of hundreds of A/cm^2 . However, explosive emission cathodes require electric fields $> 10^7 \text{ V/cm}$ and a $dE/dt > 10^{13} \text{ V/(cm s)}$ rise time in order to form explosive emission plasma at the beginning of the accelerating pulse with satisfactory cross-sectional uniformity. In addition, because of large density gradients, this plasma expands with a typical velocity of $2 \times 10^6 \text{ cm/s}$ toward the anode, causing a fast change in the diode impedance, and limiting the duration of the accelerating pulse.

Recently, a promising electron source,⁴ based on a set of carbon-epoxy capillaries, was reported that was able to produce a high current density (up to 300 A/cm^2), long duration ($\sim 450 \text{ ns}$), high energy ($\sim 200 \text{ keV}$), and uniform and reproducible cylindrical electron beam. In this paper, we report the results of experiments carried out using the same cathode in a diode powered by a 5 kJ sub-microsecond generator and producing uniform electron beams with current density up to 5 kA/cm^2 , duration up to $\sim 900 \text{ ns}$, and electron energy up to 350 keV .

II. EXPERIMENTAL SETUP

Two types of this cathode were used in these experiments: hemisphere- and strip-like cathodes (see Fig. 1). The hemisphere-like cathode was made of 300 carbon fiber-epoxy non-conductive capillaries ("Van Dijk Pultrusion Products") uniformly distributed and fixed in an aluminum cathode holder, 70 mm in diameter. The external and internal diameters of each capillary were 2 mm and 1 mm , respectively, the distance between the centers of neighboring capillaries was 3.5 mm , with the length of the capillaries decreasing toward the cathode's periphery.⁴ This cathode was used for the generation of a cylindrical electron beam. For the generation of a sheet electron beam, a 31 mm long strip-like cathode made of 12 capillaries uniformly arranged in a line was used. The length, external, and internal diameters of these capillaries were 7 mm , 1.5 mm , and 0.7 mm , respectively. When the hemisphere-like cathode was implemented, the anode was made of either a stainless steel grid (50% transparency) or a stainless steel disc 5 mm thick; when the strip-like cathode was implemented, an anode made of stainless steel with a $46 \text{ mm} \times 12 \text{ mm}$ slot was used. The cathode-anode (CA) gap was varied in the range $13\text{--}23 \text{ mm}$. In some of the experiments, a guiding magnetic field (0.085 T and 0.2 T for the hemispherical-like and strip-like cathodes, respectively) with duration of $\sim 10 \text{ ms}$, produced by Helmholtz coils, was applied.

The diode was powered by a 21-stage pulse forming network generator with stored energy of $\sim 1.8 \text{ kJ}$. The generator's operation was triggered by a Maxwell generator (model 40230) when the external magnetic field reached its maximal value. The diode voltage ϕ_{CA} , diode current I_d , and electron beam current I_b were measured using an active voltage divider, a self-integrated Rogowski coil, and a low-inductance Faraday Cup (FC), respectively. The FC, having a graphite collector 100 mm in diameter, was placed at a distance of $\sim 5 \text{ mm}$ behind the anode grid.

The light emission of the cathode plasma that is formed inside the carbon-epoxy capillaries and ejected into the CA gap (side and front views) was studied using a fast framing intensified 4Quik05A camera. For front view imaging, in

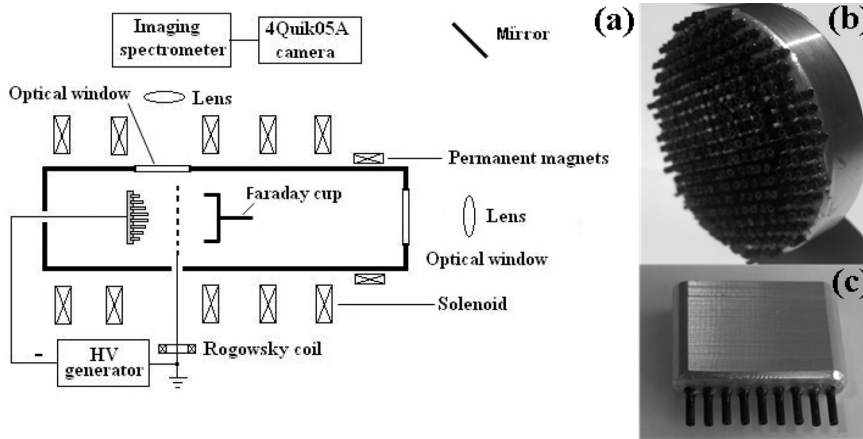


FIG. 1. (a) Experimental setup; (b) hemisphere-like cathode; (c) strip-like cathode.

order to avoid beam electrons bombarding the perspex window, two permanent magnets were installed (see, Fig. 1). The cathode plasma parameters (density, temperature, expansion velocity) were studied using visible time- and space-resolved spectroscopy. The measurements were made using a 750 mm Jobin Yvon spectrometer (2400 grooves/mm grating, spectral resolution of $\leq 0.1 \text{ \AA}/\text{pix}$). The light emission from the desired location of the plasma inside the CA gap was collected through a perspex window, and focused by a fused silica lens on the input spectrometer slit (see Fig. 1). The spectral line images at the output of the spectrometer were recorded by a 4Quik05A camera. The calibration of the optical system was carried out using “Oriol” spectral lamps.

III. EXPERIMENTAL RESULTS AND DISCUSSION

A. Parameters of the diode and generated electron beam

First, we discuss the results of the experiments with the hemisphere-like cathode. In these experiments, the change in the CA gap d_{CA} from 13 mm to 23 mm resulted in a decrease in the diode current amplitude from $\sim 18 \text{ kA}$ to $\sim 11 \text{ kA}$, with a corresponding increase in the accelerating pulse amplitude from $\sim 280 \text{ kV}$ to $\sim 450 \text{ kV}$. The duration of the accelerating pulse was $\sim 650 \text{ ns}$. In order to test this cathode with maximal current density while maintaining the accelerating voltage at $\sim 300 \text{ kV}$, the value of the CA was chosen to be $\sim 13 \text{ mm}$. Typical waveforms of the diode voltage and current, and beam current for $d_{CA} = 13 \text{ mm}$ are shown in Fig. 2. One can see that the electron emission, i.e., plasma appearance at the output of the capillaries,⁴ begins at a time delay $\tau_d \approx 15 \text{ ns}$ with respect to the beginning of the accelerating pulse when the average value of the electric field in the CA gap reaches $E_{av} \approx 26 \text{ kV/cm}$. Thus, one can expect that the surface flash-over inside the capillaries will begin at an even lower electric field.

The temporal behavior of the diode impedance shows a gradual decrease from $\sim 40 \text{ \Omega}$ at $\tau_d \approx 50 \text{ ns}$ to $\sim 10 \text{ \Omega}$ at $\tau_d \approx 550 \text{ ns}$ (see Fig. 3). Taking into account the formation and expansion of the anode plasma, one can suppose that the cathode plasma expansion is significantly smaller than $2 \times 10^6 \text{ cm/s}$, which is the typical velocity for explosive emission plasma expansion. Let us also note that at $\tau_d \approx 550 \text{ ns}$,

almost 80% of the energy stored in the generator is transferred to the energy of the electron beam, which can be considered as a rather high efficient electron beam generation.

The measurements of the electron beam by the FC showed a current amplitude of $\sim 8 \text{ kA}$, which is $\sim 85\%$ of the total diode current when one takes into account 50% transparency of the anode grid. The pattern of the electron beam on a perspex target placed at a distance of $\sim 10 \text{ cm}$ from the anode grid when a guiding magnetic field $B \approx 860 \text{ G}$ is applied is shown in Fig. 4. One can see that the diameter of the electron beam pattern with maximal intensity is $\sim 55 \text{ mm}$, which is smaller than the cathode diameter ($\sim 70 \text{ mm}$). This can be explained by the hemispherical form of the cathode, which results in a larger CA gap at the cathode periphery. Further, the injection of an electron beam with a non-compensated space charge and radius $r_b \approx 35 \text{ mm}$ into a vacuum tube with radius $r_t = 100 \text{ mm}$ and having a current

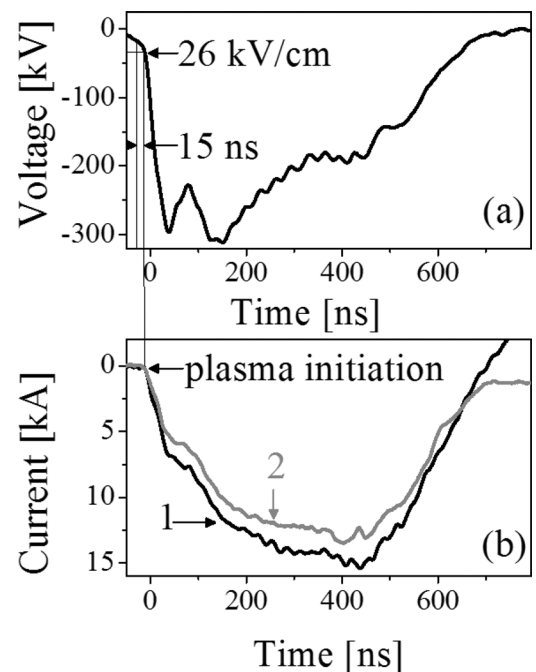


FIG. 2. Typical waveforms of the diode voltage (a) and diode (1) and electron beam (2) currents (b). $B \approx 860 \text{ G}$, $d_{CA} = 13 \text{ mm}$, distance from the anode grid up to the Faraday cup was $\approx 5 \text{ mm}$. Time delay between HV application and plasma initiation is illustrated along with the electric field at this time.

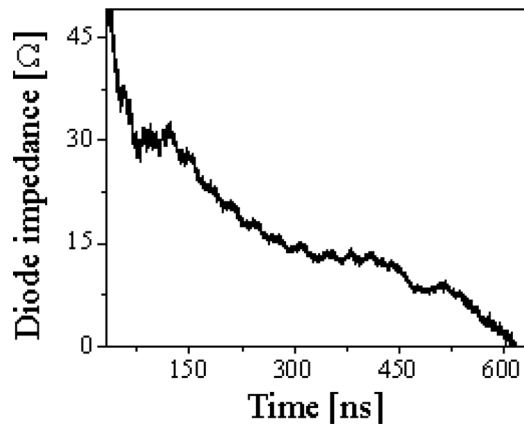


FIG. 3. Diode impedance of the carbon-epoxy capillary cathode; $\varphi_{CA} \approx 320$ kV, $d_{CA} = 13$ mm.

amplitude ($I_b \approx 8$ kA) larger than the critical current amplitude⁵ $I_{cr} = 17(\gamma^{2/3} - 1)^{3/2} / [1 + 2 \ln(r_t/r_b)] \leq 1.3$ kA should lead to the formation of a virtual cathode at a distance from the anode grid that is comparable to the value of d_{CA} . Thus, to explain the efficient transport of the electron beam, one should consider neutralization of the beam space charge by ions emitted from the anode plasma.

In addition, the operation of the multicapillary cathode and a planar grooved aluminum (Al) cathode was compared under the same experimental conditions. The Al cathode had a cylindrical form with rounded edges and concentric grooves at the emitting surface. Typical waveforms of the planar diode voltage for both cathodes obtained at $d_{CA} = 13$ mm are shown in Fig. 5. One can see that the amplitude of the voltage at the beginning of the accelerating pulse in the case of the Al cathode is larger, which is explained by a delay in the explosive plasma formation leading to mismatching of the diode and the high-voltage generator impedances. Further, using the Al cathode, the duration of the accelerating pulse is shorter by ~ 100 ns than when using the multicapillary cathode. This can be explained by the faster expansion velocity of the explosive emission plasma when the Al cathode is used.

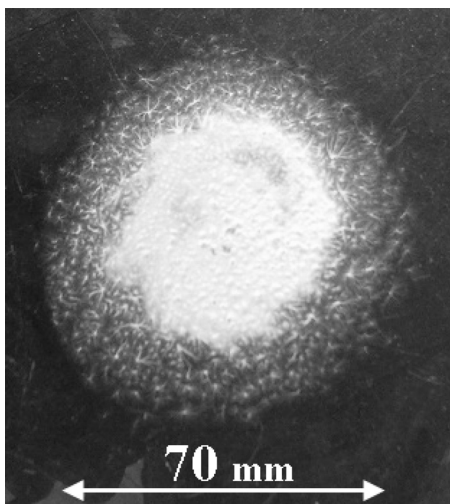


FIG. 4. Pattern of electron beam on a perspex target placed at a distance of 10 cm from the anode grid. $B \approx 860$ G, $\varphi_{CA} \approx 300$ kV, $I_d \approx 18$ kA.

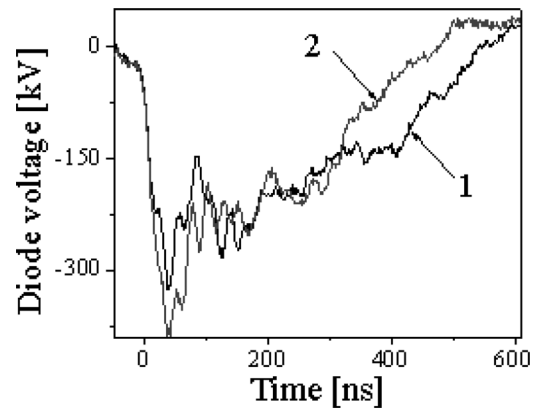


FIG. 5. Waveforms of the diode voltage: 1. Carbon-epoxy capillary cathode; 2. Al cathode. $d_{CA} = 13$ mm.

Typical front view images of the light emission from the cathode plasma obtained with the multicapillary carbon fiber-epoxy cathode and Al cathode are shown in Fig. 6. These light emission images were the same in the presence or absence of external magnetic field B . One can see a satisfactory uniform light emission from the multicapillary cathode, in contrast to the light emission from the Al cathode, where one obtains strong light emission from only one side of the cathode. These images agree qualitatively with the uniform cross-sectional distribution of the electron beam current density and longer time duration of the accelerating pulse in the case of the multicapillary cathode. Indeed, brighter plasma spots, which do not cover all the surface of the Al cathode, emit a larger current density (the maximal amplitudes of the diode current for the Al and multicapillary cathodes were approximately equal to each other), which results in the plasma having a higher temperature and larger density at that location and, respectively, in a faster plasma expansion velocity and shorter duration of the accelerating pulse. In addition, these front view images showed that the light emission from the multicapillary cathode already appears at $\tau_d = 20$ ns, whereas the bright spots emitted from the Al cathode become visible only at $\tau_d = 40$ ns. This agrees with the estimates of the average electric field of < 25 kV that is required for plasma formation when the multicapillary cathode is used, and the significant time delay in the appearance of the explosive emission plasma when the Al cathode is used.⁶

Side view light emission images from the accelerating gap at different times during the accelerating pulse are

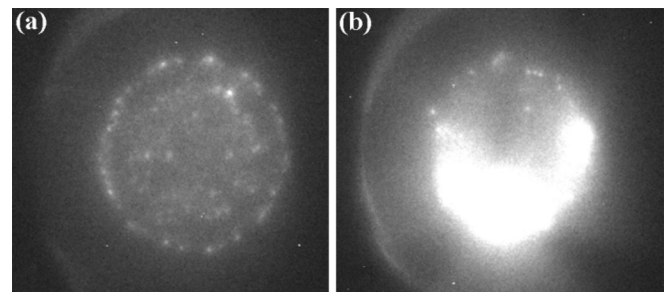


FIG. 6. Typical front view images of light emission from the (a) multicapillary carbon fiber-epoxy cathode and (b) Al cathode. $\tau_d = 500$ ns, The frame duration is of 20 ns. $B \approx 860$ G, $d_{CA} = 13$ mm, $\varphi_{CA} \approx 300$ kV.

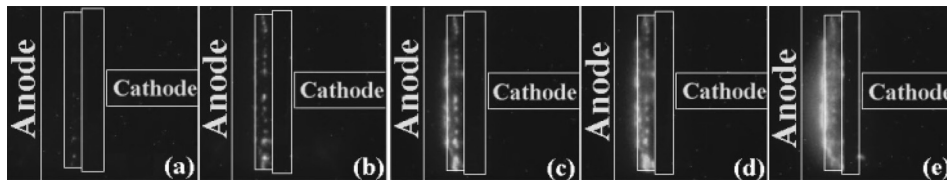


FIG. 7. Typical side images of light emission from the multicapillary carbon-epoxy cathode, (a) $\tau_d \approx 80\text{ ns}$, (b) $\tau_d \approx 150\text{ ns}$, (c) $\tau_d \approx 300\text{ ns}$, (d) $\tau_d \approx 400\text{ ns}$, (e) $\tau_d \approx 600\text{ ns}$. The frame duration is of 20 ns. $B \approx 860\text{ G}$, $d_{CA} = 13\text{ mm}$.

shown in Fig. 7. Although these images belong to different generator shots, the high reproducibility of the diode parameters allows us to regard these images as a time sequence illustration of the light emission from the CA gap during the diode's operation. One can see that the light emission from the plasma becomes visible at $\tau_d \approx 80\text{ ns}$ only on the "tips" of the capillaries. Furthermore, during the entire HV pulse, this hot dense plasma remains in the vicinity of the tips of the capillaries ($\sim 2\text{ mm}$). These data agree with the conclusions of Ref. 4, that is, the plasma formation occurs inside the capillaries due to a flashover process. Further evidence of the plasma formation inside the capillary can be seen in Fig. 8, where the light emission image was obtained at a larger magnification. The conical structure of the light outgoing from the capillary is associated with the individual plasma jet ejected from the capillary, which can be considered similar to the plasma formation inside a dielectric multicapillary cathode.^{7,8}

In addition, the side view images (see Fig. 9) show a larger light emission intensity when $B = 0$. The latter can be related to a larger volume being occupied by neutrals that are ejected from the capillaries and ionized and excited by plasma electrons, which are not magnetized in that case.

The sheet high-current electron beam was obtained using a multicapillary carbon-epoxy strip-like cathode. In order to increase the electron magnetization, in these experiments, the external magnetic field was increased up to 2 kG and the charging voltage of the high-voltage generator was decreased, which results in an accelerating voltage $\leq 250\text{ kV}$

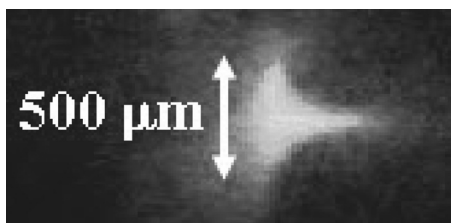


FIG. 8. Plasma jet ejection from carbon fiber-epoxy capillary.

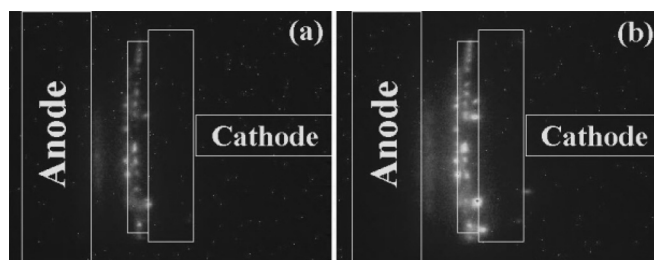


FIG. 9. Side view images of light emission from the multicapillary carbon-epoxy cathode, both images are taken at similar times (close to the middle of the HV pulse). (a) With an applied external magnetic field; (b) without an applied external magnetic field.

at $d_{CA} = 13\text{ mm}$. A pattern of the beam (see Fig. 10) obtained on a stainless steel plate placed at a distance of 10 mm from the anode slot, shows that the cross-sectional area where one obtains the maximal intensity of the pattern is rectangular in form. The duration of the accelerating pulse in these experiments increases up to 900 ns with the amplitude of the electron beam reaching 6 kA. This allows one to state that this type of cathode can be used for the generation of an electron beam with a current density of several kA/cm^2 at moderate accelerating voltages and without shorting of the CA gap by the cathode plasma.

In the present experiments, we did not test the longevity of these cathodes. Nevertheless, both types of cathode operated without any deterioration in their emission properties, for several hundreds of generator shots, in spite of the large current density (up to $10^5\text{ A}/\text{cm}^2$) through each capillary.

B. Spectroscopic studies of the cathode plasma

Spectral lines emitted from plasma neutrals (H_α and H_β) and ions (CII 4267.26 Å) were recorded for four different positions inside the CA gap, from close to the edge ($\sim 200\text{ }\mu\text{m}$) of the capillaries, to 5 mm away from them, i.e., close to the middle of the CA gap. In order to obtain a reliable profile of the spectral line, the input slit of the spectrometer was set to $100\text{ }\mu\text{m}$, and the exposure time of the intensified framing camera was set to 100 ns.

In order to determine the plasma expansion velocity for hydrogen atoms and carbon ions, a time delay in the appearance of spectral lines obtained at different distances from the cathode was applied. It was found that the velocity of C II ions and H I atoms does not exceed 1.5×10^6 . These data were obtained in the vicinity of the cathode because of the drastic decrease in all the spectral line intensities versus the distance from the cathode. That is, at a distance of 5 mm, hydrogen spectral lines were not obtained and the intensity of the strongest C II spectral line also was negligibly small. These data indicate a rapid decrease in the density of the cathode plasma versus the distance from the cathode, which agrees with the light image results, which show that the

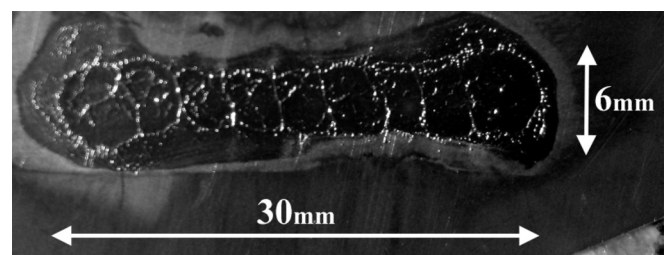


FIG. 10. Pattern of the sheet beam on stainless steel. $\varphi_{CA} \approx 250\text{ kV}$, $I_d \approx 6\text{ kA}$, $B \approx 2\text{ kG}$.

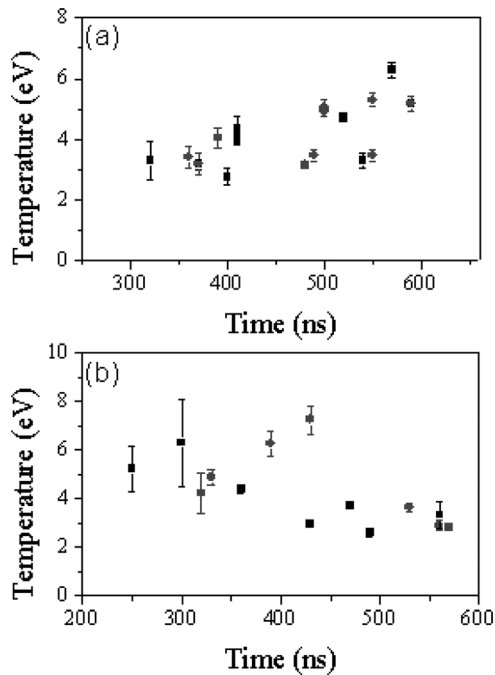


FIG. 11. Temperature evolution of C II ions (a) and hydrogen atoms (b) at a distance of 0.2 mm from the tips of the capillaries. Light circles: $B = 0$. Dark rectangles: $B \approx 860$ G.

dense cathode plasma remains within the vicinity of the cathode throughout the HV pulse.

The temperature of plasma CII ions and hydrogen atoms was studied using the Doppler broadening analysis of the 4267.26 \AA and H_{α} spectral lines. The latter is significantly less sensitive to the Stark effect than the H_{β} line.^{9,10} The results of this analysis (see Fig. 11) show no difference in the temperatures of plasma particles, $T_H \approx T_{CII} = 4 \pm 1$ eV, for both $B = 0$ and $B \approx 860$ G. The same temperature values were obtained for other distances (up to 5 mm) from the cathode. These results indicate thermal equilibrium between plasma neutral and ions, which can be realized inside the capillary where the plasma density can be significantly larger than outside the capillary.

Using the instrumental and Doppler broadening of the H_{α} spectral line, the FWHM of the Stark broadening of the H_{β} spectral line was determined and used to calculate the plasma electron density. In these calculations, the effects of electron impact and ion dynamics were neglected, which can be considered reasonable assumptions for plasma whose density and temperature are $< 10^{15} \text{ cm}^{-3}$ and $T < 5$ eV, respectively.⁹ Using the analysis method presented in Ref. 10, the plasma electron density was determined at $\tau_d \approx 350$ ns, i.e., in the middle of the accelerating pulse, when the intensity of the H_{β} spectral line was maximal, resulting in a small error in the fitting process. The results of this analysis are shown in Fig. 12. At distances from the cathode of more than 3 mm, the intensity of the H_{β} spectral line was too low to determine its FWHM with reasonable certainty, because of the relatively small signal to noise ratio. One can see that the plasma density decreases in an exponential-like manner. This result agrees well with the former conclusions about the rapid decrease in the plasma density across the CA gap.

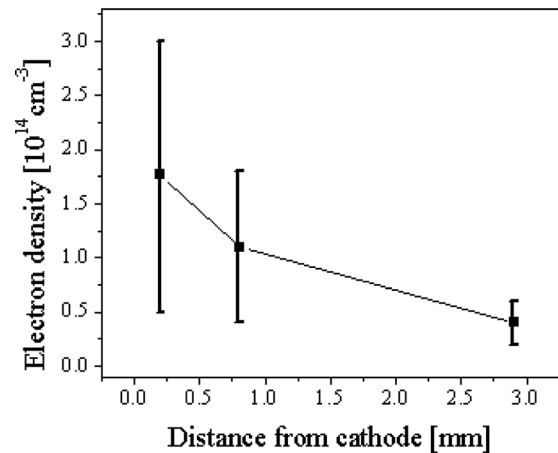


FIG. 12. Plasma electron density (range of obtained values) versus the distance from the cathode at $\tau_d \approx 350$ ns.

IV. SUMMARY

The experiments showed that the multicapillary carbon-epoxy cathode described and tested at electron current densities up to 300 A/cm^2 in Ref. 4 can be used also to generate reliably electron beams with a current density up to several kA/cm^2 at moderate accelerating voltages of ≤ 350 kV, pulse duration of up to $\sim 1 \mu\text{s}$, and with a satisfactory uniform cross-sectional distribution of the electron beam current density. The cathode plasma, serving as a source of electrons, is produced by a flashover process inside the capillaries. Depending on the form of the cathode, one can generate electron beams with the required cross section. The multicapillary cathode showed a significant improvement as compared to explosive emission cathodes in terms of the emission centers' distribution uniformity, duration of the accelerating pulse, and fast (< 20 ns) turn-on even at a moderate electric field rise time. As compared with the commonly used carbon- and velvet fiber-based cathode, the operation of which is also characterized by flashover plasma formation, this type of cathode has a significant advantage: a long lifetime operation without degradation of emission properties at current densities of several kA/cm^2 .

¹G. A. Mesyats, *Explosive Electron Emission* (URO, Ekaterinburg, 1998).

²E. Oks, *Plasma Cathode Electron Sources: Physics Technology, Applications* (Wiley-VCH, Berlin, 2006).

³Ya. E. Krasik, D. Yarmolich, J. Z. Gleizer, V. Vekselman, Y. Hadas, V. Tz. Gurovich, and J. Felsteiner, "Pulsed electron sources," *Phys. Plasmas* **16**, 057103 (2009).

⁴J. Z. Gleizer, T. Queller, Yu. Bliokh, S. Yatom, V. Vekselman, Ya. E. Krasik, and V. Bernshtam, *J. Appl. Phys.* **112**, 023303 (2012).

⁵L. S. Bogdankevich and A. A. Ruchadze, *Sov. Phys. Usp.* **14**, 163 (1971).

⁶Ya. E. Krasik, A. Dunaevsky, A. Krokhmal, J. Felsteiner, A. V. Gunin, I. V. Pegel, and S. D. Korovin, *J. Appl. Phys.* **89**, 2379 (2001).

⁷M. Friedman, M. Myers, F. Hegeler, S. B. Swaneckamp, J. D. Sethian, and L. Ludekingd, *Appl. Phys. Lett.* **82**, 179 (2003).

⁸J. Z. Gleizer, Y. Hadas, D. Yarmolich, J. Felsteiner, and Ya. E. Krasik, *Appl. Phys. Lett.* **90**, 181501 (2007).

⁹H. R. Griem, *Spectral Line Broadening by Plasma* (Academic, New York, 1974).

¹⁰M. A. Gigosos, M. A. Gonzalez, and V. Cardenoso, *Spectrochim. Acta, Part B* **58**, 1489 (2003).